Available online at www.sciencedirect.com

SCIENCE DIRECT®

Bioelectrochemistry 66 (2005) 41–47

Bioelectrochemistry

www.elsevier.com/locate/bioelechem

TiO_2 phytate films as hosts and conduits for cytochrome *c* electrochemistry

Katy J. McKenzie[a], Frank Marken[a,*], Marcin Opallo[b]

[a]*Department of Chemistry, Loughborough University, Loughborough, Leicestershire, LE11 3TU, UK*
[b]*Institute of Physical Chemistry, Polish Academy of Sciences, ul. Kasprzaka 44/52, 01-224 Warszawa, Poland*

Received 6 December 2003; received in revised form 24 March 2004; accepted 31 March 2004
Available online 21 August 2004

Abstract

Cytochrome *c* is accumulated into a film of TiO_2 nanoparticles and phytate by adsorption from an aqueous solution into the mesoporous structure. Stable voltammetric responses and high concentrations of redox protein within the TiO_2 phytate layer can be achieved. Two types of electrode systems are reported with (i) the modified TiO_2 phytate film between electrode and aqueous solution phase and (ii) the modified TiO_2 phytate film buried under a porous gold electrode ('porotrode').

The electrical conductivity of TiO_2 phytate films is measured and compared in the dry and in the wet state. Although in the dry state essentially insulating, the TiO_2 phytate film turns into an electrical conductor (with approximately 4 Ω cm specific resistivity assuming ohmic behaviour) when immersed in aqueous 0.1 M phosphate buffer solution at pH 7. The redox protein cytochrome *c* is therefore directly connected to the electrode via diffusion and migration of electrons in the three dimensional mesoporous TiO_2 phytate host structure. Electron transfer from cytochrome *c* to TiO_2 is proposed to be the rate-determining step for this conduction mechanism.

Keywords: Cytochrome *c*; Process in Biochemistry; Bioelectrochemistry; Titania nanoparticles; Electron hopping; Sensors

1. Introduction

Mesoporous oxides in the form of thin films are relatively stable in aqueous environments and are versatile for a wide range of applications in sensors [1], as electrocatalysts [2], and for modified electrodes [3]. Considerable interest in TiO_2 films exists predominantly due to their application in hydrophilic coatings [4], in photovoltaic cells [5], as photocatalysts [6], and as pigments [7]. There have also been several previous reports on the immobilisation of biological redox systems such as oligonucleotides and DNA [8], heme proteins [9] or redox enzymes [10] in titanium dioxide [11–13] and other metal oxide hosts such as manganese dioxide [14] and tin dioxide [15]. By combining a rigid host structure, prepared for example from metal oxide nanoparticles of appropriate size, and a more fragile biological system, novel functional composite materials can be obtained [16]. In this report TiO_2 is combined with cytochrome *c* and it is shown that in addition to providing a rigid host structure, metal oxides can also contribute to the efficient transport of electrons.

The heme protein cytochrome *c* has been coupled successfully to electrode surfaces by Hill et al. [17]. Over the past two decades, this redox protein of 12 kD mass and approximately 3.7 nm size [18] has often been considered as a model system for biological electron transfer [19] and for bioelectrocatalysis [20]. The most prominent feature of the almost spherical cytochrome *c* structure is a strongly positively charged lysine rich region on the outer shell of the protein, which is responsible for docking to electron donor and acceptor sites with complementary negative surface charge [21]. A wide range of films with negative surface functionalities, e.g. carboxylate functionalised surfaces [22], polysulfonates [23], polyphosphate (DNA) modified surfaces [24], and dialysis membranes [25] have

* Corresponding author. Tel.: +44 1509 222 551; fax: +44 1509 223 925.
E-mail address: f.marken@lboro.ac.uk (F. Marken).

1567-5394/$ - see front matter © 2004 Elsevier B.V. All rights reserved.
doi:10.1016/j.bioelechem.2004.03.008

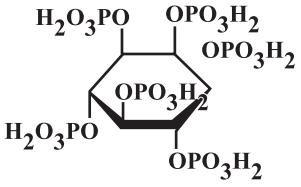

Scheme 1.

been proposed for reversibly docking cytochrome *c* and related heme proteins for applications in bioelectrochemistry and in biosensing. A recent monograph summarises developments in this field [26].

We have shown that cytochrome *c* is strongly adsorbed from aqueous solution into thin films of TiO_2 nanoparticles assembled with the help of phytic acid (see Scheme 1) 'binder' molecules [27]. After immersion of the TiO_2 phytate film coated onto tin-doped indium oxide (ITO) electrode surfaces, high concentrations of the redox protein in a stable and active state are immobilised. Increasing the film thickness in a layer-by-layer manner increases the amount of adsorbed redox active protein [27] and therefore improves the electrochemical response. This three-dimensional binding of the redox protein to the electrode surface was rationalised by a transport process similar to diffusion with either protein diffusion, electron hopping from site to site within the mesoporous film, or both occurring simultaneously [27].

In this report it is shown that TiO_2 phytate films, although electrically insulating in the dry state, conduct electrons when immersed in aqueous buffer solution. The resulting conductivity within the film is sufficient to explain the three-dimensional coupling of the redox protein cytochrome *c* to the electrode surface without the need of protein diffusion. It is also shown that the TiO_2 phytate films may be deposited onto plain non-conducting glass surfaces and then sputter-coated with a porous gold layer. The resulting 'buried' modified electrode (or 'porotrode') is cheap, readily prepared on a variety of substrates, electrochemically active similar to conventional modified ITO electrodes, and allows cytochrome *c* electrochemistry to be observed.

2. Experimental

2.1. Instrumentation

Electrochemical measurements were performed with a Eco Chemie PGSTAT20 Autolab bipotentiostat system. Conventional voltammetric experiments were conducted in staircase voltammetry mode and with a platinum gauze counter and saturated calomel reference electrode (SCE, Radiometer). The working electrode was either a modified glass microscope slide (13×75 mm, Fisher Scientific, UK) or tin-doped indium oxide (ITO) coated glass (9m×60 mm, resistivity 20 $\Omega\ \square^{-1}$) obtained from Image Optics Components (Basildon, Essex). Prior to conducting experiments, all solutions were purged with argon (BOC, UK). All experiments were carried out at a temperature of 22±2 °C.

Film conductivity measurements in dry and wet state were performed in a two- or four-electrode arrangement, respectively, with a second working electrode controlled in bipotentiostatic mode (vide infra). Scanning electron microscopy images were obtained with a Leo 1530 Field Emission Gun Scanning Electron Microscope system. Prior to SEM imaging, the sample surface was scratched with a scalpel blade.

2.2. Chemical reagents

Titania sol (anatase, ca. 6 nm diameter, 30–35% in aqueous HNO_3, pH 0–3) was obtained from Tayca, Osaka, Japan and diluted 100-fold with deionised water. $[Ru(NH_3)_6]Cl_3$ (Johnson Matthey), Horse heart cytochrome *c* (type VI, Sigma, molecular weight 12384 g mol^{-1}), $HClO_4$ (60%), KCl, KH_2PO_4, K_2HPO_4, phytic acid dodecasodium salt hydrate [*myo*-inositol hexakis (dihydrogen phosphate) dodecasodium salt], and 3-mercaptopropionic acid (Aldrich) were obtained commercially. Demineralised and filtered water was taken from an Elga water purification system (Elga, High Wycombe, Bucks, UK) with a resistivity of not less than 18 MΩ cm.

2.3. Electrode design

Films of TiO_2 phytate were deposited following a layer-by-layer dip coating strategy [28]. A clean glass or ITO surface (washed with ethanol and water, dried, and 30 min heat treated at 500 °C in air) is dipped into a colloidal solution of TiO_2 nanoparticles followed by rinsing. The surface charge of the resulting nanoparticle deposit is reversed by dipping into a solution of phytic acid (40 mM in pH 3 aqueous solution) followed by rinsing. The process, which is carried out by a robotic Nima dip coating carousel (DSG-Carousel, Nima Technology, Coventry, UK), can be repeated and results in a thickness increase of the TiO_2 phytate deposit of approximately 30 nm per layer [27]. Oxide films formed in this way are stable in air and may be stored under ambient conditions.

Gold coatings with 20 or 40 nm thickness were applied by sputter-coating (Polaron E5150 SEM gold sputter coating unit). A typical electrode cross section is shown in Fig. 1A. The electrode surface was scratched with a scalpel blade and the exposed oxide film between ITO substrate and gold coating can clearly be seen. The gold coating appeared porous (see Fig. 1B) even when 40 nm thick. The porous nature of the gold coating is probably due to the topography of the underlying oxide film.

2.4. Conductivity measurements

Conductivity measurements of thin TiO_2 phytate films were carried in dry and in wet state. Earlier measurements

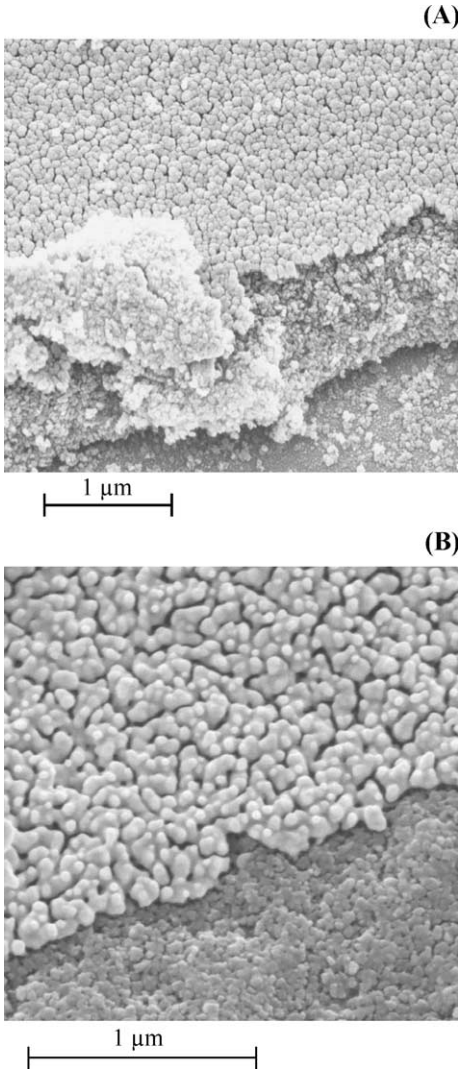

Fig. 1. FEGSEM images of (A) a 30 layer coating of TiO_2 phytate on a glass substrate sputter-coated with a film of 40 nm gold and (B) a porous 40 nm gold film on the mesoporous oxide film at higher magnification.

employing conducting AFM techniques [29] clearly indicated essentially insulating behaviour in the dry state. However, based on the known semiconducting properties of TiO_2 [30] some degree of electrical conductivity was expected. In a

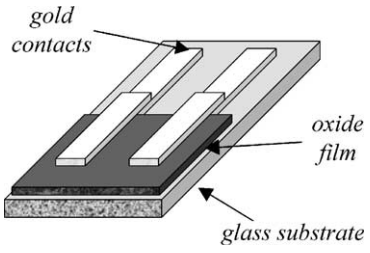

Fig. 2. Schematic drawing of the device used for conductivity measurements in aqueous solution environments. Two gold contacts sputter coated onto a 30-layer TiO_2 phytate film on glass were employed as working electrode 1 and working electrode 2 in a bipotentiostatic system.

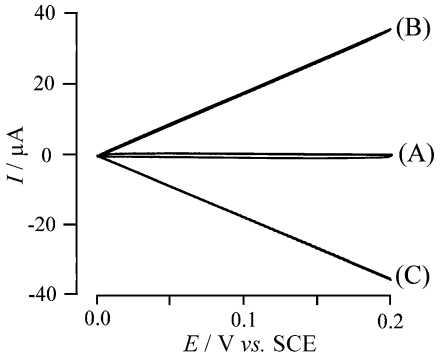

Fig. 3. Cyclic voltammograms (scan rate 20 mV s^{-1}) obtained with a conductivity probe (glass slide coated with 30 layers TiO_2 phytate with two gold contacts) immersed in aqueous 0.1 M phosphate buffer solution at pH 7. (A) Only working electrode 1 is connected and the potential applied to the electrode is scanned from 0.0 V vs. SCE to +0.2 V vs. SCE. (B, C) Working electrode 1 with the potential applied to the electrode scanned from 0.0 V vs. SCE to +0.2 V vs. SCE and working electrode 2 with the potential held at 0.0 V vs. SCE. The experiment was conducted in bipotentiostatic mode and currents (B) and (C) correspond to responses observed at working electrode 1 and working electrode 2, respectively.

recent literature report humidity dependent conductivity of titania thin films was observed [31]. Also, in photovoltaic cells transport of electrons in dye-modified mesoporous TiO_2 films has been reported to follow a diffusion type mechanism [32].

A conductivity probe was prepared by gold sputter coating contacts onto the surface of the TiO_2 phytate film to give two symmetric electrodes (see Fig. 2A). The gap between the two gold contacts was typically 2 mm and the length of the probes on the oxide layer 12 mm. The conductivity of the TiO_2 phytate film (30 layers) in dry state was determined via two probe measurement and found to be extremely low consistent with earlier reports [29]. However, a dramatic change occurred in aqueous solution environments. Measurements in phosphate buffer solution (0.1 M, pH 7) were conducted in bipotentiostatic mode. The two gold contacts on the oxide film were connected as working electrode 1 and working electrode 2, and their potential was controlled versus a saturated Calomel reference electrode and with a Pt gauze counter electrode. In this experimental arrangement well-defined potentials are applied at the two working electrodes. Typical current responses detected at working electrodes 1 and 2 are shown in Fig. 3.

3. Results and discussion

3.1. The reduction of $Ru(NH_3)_6^{3+}$ at TiO_2 phytate modified electrodes and porotrodes

$Ru(NH_3)_6^{3+}$ is readily adsorbed and accumulated into TiO_2 phytate films. It has been shown recently that characteristically enhanced and film thickness dependent voltammetric responses for the one electron reduction

(Eqs. (1) and (2)) are detected at modified ITO, gold [33], or platinum electrodes [29].

$$Ru(NH_3)_6^{3+}(aq) + e^- \rightarrow Ru(NH_3)_6^{2+}(aq) \quad (1)$$

$$Ru(NH_3)_6^{3+}(ads) + e^- \rightarrow Ru(NH_3)_6^{2+}(aq) \quad (2)$$

Fig. 4A shows both the voltammogram obtained for the reduction of 1 mM $Ru(NH_3)_6^{3+}$ in aqueous 0.1 M KCl at a bare and at a modified ITO electrode. A reversible reduction response consistent with the solution phase process (Eq. (1)) occurs at E_{mid}=−0.18 V vs. SCE. In the presence of the TiO_2 phytate film a new more pronounced response is detected. Fig. 4A shows the voltammetric response observed for a 15-layer TiO_2 phytate modified ITO electrode immersed first in 1 mM $Ru(NH_3)_6^{3+}$, then rinsed and re-immersed into clean aqueous 0.1 M KCl. The voltammetric response for the reduction of adsorbed $Ru(NH_3)_6^{3+}$ (Eq. (2)) is detected at E_{mid}=−0.32 V vs. SCE (see Fig. 4A). The difference in peak currents, I_p^{red} and I_p^{ox}, for this voltammetric response is due to the desorption of $Ru(NH_3)_6^{2+}$ and loss into the solution phase.

The voltammetric characteristics are investigated next for the 'porotrode' case, in which the TiO_2 phytate film is deposited onto a non-conducting glass substrate and then sputter-coated with a porous but electrically conducting

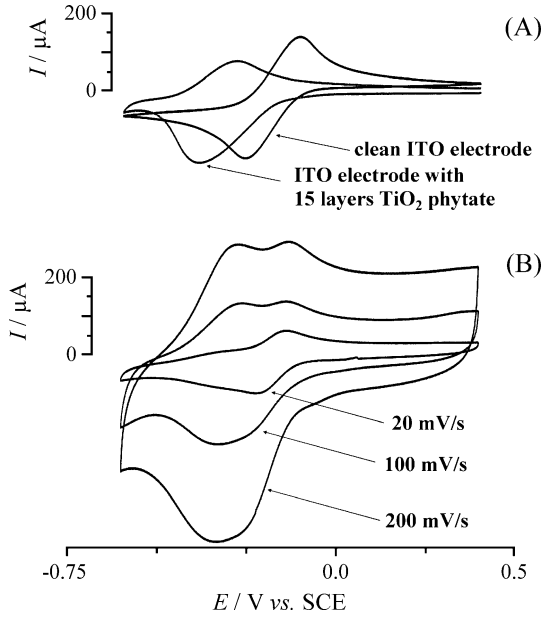

Fig. 4. (A) Cyclic voltammograms (scan rate 100 mV s^{-1}) for a bare ITO electrode (area 7×7 mm) immersed in 1 mM $[Ru(NH_3)_6]^{3+}$ in 0.1 M KCl, and for an ITO electrode (area 7×7 mm) coated with 15 layers TiO_2 phytate. Prior to recording cyclic voltammograms in 0.1 M KCl, the coated electrode was dipped into 1 mM $[Ru(NH_3)_6]^{3+}$ in 0.1 M KCl for one minute, and rinsed with deionised water. (B) Cyclic voltammograms (different scan rates as shown) for 15 layers TiO_2 phytate film sputter-coated with 40 nm gold (area 7×7 mm). The 'porotrode' was dipped into aqueous 40 mM phytic acid solution (pH 3) and rinsed with deionised water prior to recording cyclic voltammograms in aqueous 1 mM $[Ru(NH_3)_6]^{3+}$ in 0.1 M KCl.

gold film. In Fig. 4B typical voltammograms for the reduction of 1 mM $Ru(NH_3)_6^{3+}$ in aqueous 0.1 M KCl are shown. The capacitive background current is considerably enhanced due to the porous nature of the gold coating. It can be seen that two distinct voltammetric responses at E_{mid}=−0.18 V vs. SCE and at E_{mid}=−0.32 V vs. SCE are observed. From the difference in scan rate dependence of the two signals it can be concluded that the first reduction is consistent with a solution phase redox system (Eq. (1); the peak current is proportional to the square root of scan rate) and the second reduction is consistent with an immobilised redox system (Eq. (2); the peak current is proportional directly to the scan rate). The reduction response for the immobilised redox couple scales approximately linear with film thickness up to at least 15-layer deposits.

3.2. The reduction of cytochrome c at TiO_2 phytate modified electrodes and porotrodes

Cytochrome *c* is readily accumulated and immobilised in TiO_2 phytate films [27]. It has been shown that high concentrations of the redox protein and stable electrode characteristics can be achieved. Fig. 5A shows a typical voltammetric response for the reduction of 50 µM cytochrome *c* in aqueous 0.1 M phosphate buffer solution at a ITO electrode modified with 10 layers of TiO_2 phytate (ca. 300 nm thickness). A well-defined reduction response with E_{mid}=0.01 V vs. SCE is detected. The peak current of I_p=1.14 µA is orders of magnitude higher than that expected for a diffusion controlled reduction response (I_p^{red}=21 nA, based on the Randles-Sevcik expression [34] and a diffusion coefficient of cytochrome *c* in water, $D_{cytc,solution}=(6\pm2)\times10^{-11}$ m^2 s^{-1} [35]). Therefore this reduction process is dominated by cytochrome *c* immobilised in the TiO_2 phytate film (Eq. (3)).

$$Fe(III)Cyt\ c(ads) + e^- \rightarrow Fe(II)Cyt\ c\ (ads). \quad (3)$$

The permanent immobilisation of cytochrome *c* is confirmed when the electrode is removed from the solution, rinsed with water, and re-immersed in clean electrolyte solution (aqueous 0.1 M phosphate buffer, pH 7). The reduction response for the cytochrome *c* remains stable [27]. The voltammetric response for the reduction of cytochrome *c* has been shown to scale linearly with film thickness (at sufficiently low scan rates) and with the concentration of cytochrome *c* in solution during the adsorption step [27]. The peak currents shown in Fig. 5A increase approximately linearly with scan rate for 2, 5, and 10 mV s^{-1} and therefore are indicative of complete electrolysis of a thin film of material. From the charge under the voltammetric response the concentration of cytochrome *c* in the film, 1.4 mM, can be estimated (assuming a 300-nm thickness). However for thicker film deposits (and for higher scan rates) diffusion control is observed [27]. The approximate diffusion coefficient for the transport within the film $D_{cytc,\ membrane}$=

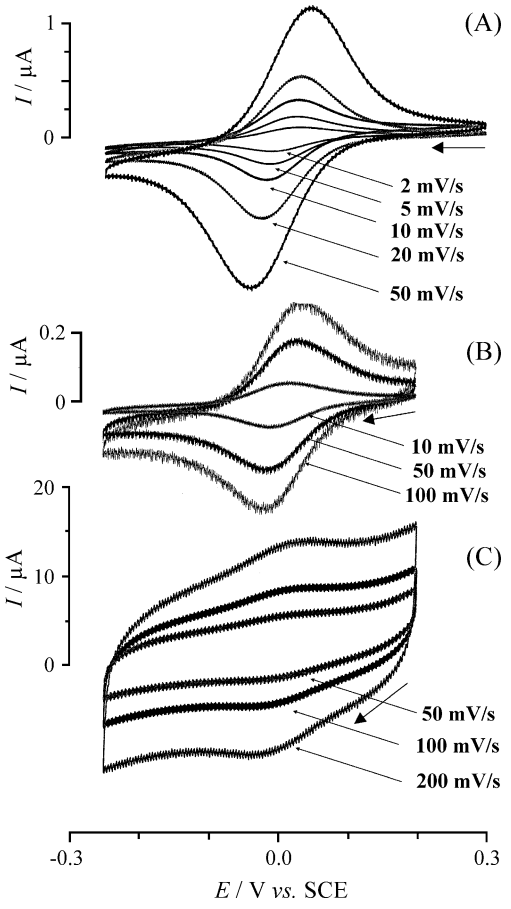

Fig. 5. (A) Cyclic voltammograms (different scan rates as shown) for an ITO electrode (area 9×9 mm) coated with 10 layers TiO_2 phytate and immersed in 0.05 mM cytochrome *c* in aqueous 0.1 M phosphate buffer solution (pH 7). (B) Cyclic voltammograms (different scan rates as shown) for a 2-mm diameter gold electrode coated with a monolayer of mercaptopropionic acid and with 10 layers TiO_2 phytate and immersed in 0.05 mM cytochrome *c* in aqueous 0.1 M phosphate buffer solution (pH 7). (C) Cyclic voltammograms (different scan rates as shown) for a 60-layer TiO_2 phytate film sputter-coated with a 20 nm Au film (area 7×7 mm). Prior to immersion of the porotrode in 0.2 mM cytochrome *c* in aqueous 0.1 M phosphate buffer (pH 7) for 10 min, the porotrode was dipped in 3-mercaptopropionic acid in aqueous 0.1 M phosphate buffer solution (pH 7) rinsed with water, then dipped into aqueous 40 mM phytic acid solution (pH 3) and rinsed with water. Cyclic voltammograms were recorded in clean aqueous 0.1 M phosphate buffer solution at pH 7 containing no cytochrome *c*.

2×10^{-14} m^2 s^{-1} [27] was reported and based on this, the scan rate for the transition from 'thin film' behaviour to diffusion characteristics can be predicted (Eq. (4)).

$$v = \frac{DRT}{\delta^2 F} \approx 0.005\text{V s}^{-1} \quad (4)$$

In this equation the scan rate v for the transition is obtained from the diffusion coefficient, D, the gas constant, R, the temperature, T, the film thickness, δ, and the Faraday constant, F. Thus, diffusion controlled voltammetric responses are expected for film thicker than 300 nm and for scan rates higher than approximately 50 mV s^{-1}. Fig. 6 shows a diagram indicating the characteristic zones for complete electrolysis (zone E) and for diffusion control (zone D).

For the cytochrome *c* redox process, gold electrodes coated with 3-mercaptopropionic acid and modified with TiO_2 phytate films exhibit essentially the same voltammetric characteristics when compared to those observed at ITO electrodes. The 3-mercaptopropionic acid binder provides a stable bond between gold surface and the membrane and prevents protein from denaturing and blocking the electrode surface. Fig. 5B shows typical voltammograms obtained with a 10-layer deposit of TiO_2 phytate at a 2-mm diameter gold disc electrode immersed in 50 µM cytochrome *c* in 0.1 M phosphate buffer solution at pH 7.

Also in the 'porotrode' geometry (the TiO_2 phytate film is located between a non-conducting glass substrate and a porous gold coating, see Fig. 1), voltammetric responses for the reduction of cytochrome *c* are detected. The porosity of the sputter-coated gold layer causes a considerable capacitive back ground current (see Fig. 5C) but the reduction and re-oxidation of cytochrome *c* with E_{mid}=0.0 V vs. SCE are clearly detected. For the voltammograms shown in Fig. 5C a 60-layer TiO_2 phytate film coated with a 20-nm gold film was employed. The electrode was pretreated by (i) coating the gold with 3-mercaptopropionic acid (to avoid irreversible adsorption of protein onto the gold surface), (ii) dipping into phytic acid (to re-equilibrate the composition and pH of the membrane), and (iii) by 10-min immersion of the electrode in 0.05–0.2 mM cytochrome *c* in aqueous 0.1 M phosphate buffer at pH 7. After rinsing and transfer of the electrode into clean buffer solution without cytochrome *c*, voltammograms at different scan rates were recorded. Experiments with different cytochrome *c* concentrations revealed an approximately linear dependence of the peak current on the amount of immobilised protein. Experiments with different thicknesses of the TiO_2 phytate film revealed that the reduction response for cytochrome *c* does not increase beyond a film of approximately 20–30 layers at a scan rate of 50 mV s^{-1}. This observation is consistent with diffusion control as predicted in Fig. 6.

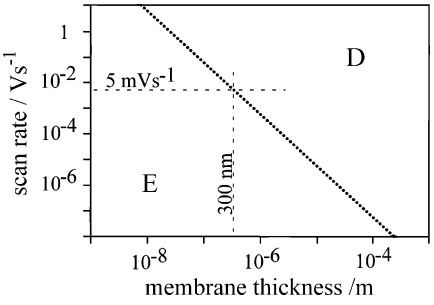

Fig. 6. Plot of the scan rate versus the membrane thickness (see Eq. (4)). The dotted line indicates the transition from complete electrolysis (zone E) to diffusion control (zone D) and has been drawn assuming a diffusion coefficient of $D_{cytc,membrane}=2\times10^{-14}$ m^2s^{-1} and T=298 K.

3.3. The diffusion–conduction mechanism for redox processes at TiO_2 phytate modified electrodes and porotrodes

It is interesting to further investigate and discuss the diffusion process within wet TiO_2 phytate membranes in the absence and in the presence of cytochrome *c*. Diffusion of the immobilised protein appears not very likely and especially at high concentrations of cytochrome *c* the electron hopping process should dominate. The effective diffusion coefficient for this process has been previously estimated as $D_{cytc,membrane}=2\times10^{-14}$ m^2 s^{-1} [27]. An estimate for the apparent diffusion coefficient for the electrons can be obtained from conductivity measurements.

Fig. 3 shows voltammetric data obtained for a 30 layer TiO_2 phytate film (ca. 900 nm thickness, 2 mm width, 12 mm length). The background voltammograms obtained for both gold electrodes independently are identical and consistent with capacitive charging (see Fig. 3A). When gold electrode 2 is held at 0.0 V vs. SCE and the potential applied to gold electrode 1 is scanned from 0.0 to +0.2 V vs. SCE, a symmetric ohmic current response is observed (see Fig. 3B and C, respectively). From this current response and from the known thickness and dimensions of the film the specific resistivity of the TiO_2 phytate in aqueous 0.1 M phosphate buffer at pH 7 can be estimated as 4 Ω cm. This value plausible but is low compared to literature values for pure TiO_2 nanoparticle films [36]. However, the materials studied and conditions were different.

The apparent diffusion coefficient for electrons, D_e, in the TiO_2 phytate membrane immersed in aqueous phosphate buffer at pH 7 can be estimated from the mobility, u_e, the Faraday constant, *F*, the gas constant, *R*, and the temperature, *T* (Eq. (5)) or from the measured specific resistivity, ρ=4 Ω cm (see Experimental), the electron charge, e, and the concentration of charge carriers, *n* (here assumed to be one per particle).

$$D_e = \frac{RT}{F}u_e = \frac{RT}{F}\frac{1}{\rho e n}. \quad (5)$$

The order of magnitude estimate obtained for the electron diffusion coefficient is $D_e=10^{-6}$ m^2 s^{-1} (which seems reasonable when compared with literature reports [37]) and therefore significantly faster compared to the observed transport of electrons in the presence of cytochrome *c*, $D_{cytc,\ membrane}=2\times10^{-14}$ m^2 s^{-1} [27]. It can be concluded that cytochrome *c* acts as trapping state in the TiO_2 host and the electron transfer from cytochrome *c* to TiO_2 is rate limiting. The experiment shown in Fig. 3 was repeated after immersion of the conductivity probe into a solution of 0.2 mM cytochrome *c* in aqueous 0.1 M phosphate buffer at pH 7. In the presence of cytochrome *c* adsorbed into the TiO_2 phytate membrane the conductivity drops by approximately one order of magnitude. This result supports the hypothesis of cytochrome *c* and TiO_2 acting as trapping state and conduit, respectively. Further work will be required to quantify and exploit this conductivity effect.

4. Conclusions

Two geometries for modified electrodes (surface modified and substrate modified) have been employed for the electrochemistry of an immobilised redox protein, cytochrome *c*. A mesoporous structure formed via layer-by-layer deposition, TiO_2 phytate, has been employed for the accumulation and immobilisation process. The specific resistivity of the mesoporous TiO_2 phytate film has been determined in aqueous phosphate buffer solution at pH 7 and the transport mechanism identified as predominantly electronic. Additional contributions to the observed currents from protein diffusion or from direct inter-protein electron hopping are possible. Factors governing this electronic conduction process are under further investigation. When compared to other fully electrically conducting or to fully insulating host materials, mesoporous TiO_2 phytate offers considerable advantages, one of which is the known biocompatibility of titania. It appears likely that for the immobilisation and redox cycling of sensitive biological systems similar to cytochrome *c*, mesoporous TiO_2 phytate is beneficial as a host and as electronic conduit.

Acknowledgements

F.M. thanks the Royal Society for a University Research Fellowship. K.J.M. thanks the EPSRC for a studentship, Support from the British Council (Research Partnership Programme Grant Project No. 248) is gratefully acknowledged.

References

[1] a P.T. Moseley, J.O.W. Norris, D.E. Williams, Techniques and Mechanisms in Gas Sensing, Adam Hilger, Bristol, 1991;
b R. Ramamoorthy, P.K. Dutta, S.A. Akbar, Oxygen sensors: materials, methods, designs and applications, J. Mater. Sci. 38 (2003) 4271–4282 (See for example).
[2] H. Wendt, G. Kreysa, Electrochemical Engineering, Science, and Technology in Chemical and Other Industries, Springer, Berlin, 1999.
[3] a A. Walcarius, M. Etienne, S. Sayen, B. Lebeau, Grafted silicas in electroanalysis: amorphous versus ordered mesoporous materials, Electroanalysis 15 (2003) 414–421 (See for example);
b C.A.C. Sequeira, M.J. Hudson (Eds.), Multifunctional Mesoporous Inorganic Solids, Kluwer, Dordrecht, 1993.
[4] K.S. Guan, B.J. Lu, Y.S. Yin, Enhanced effect and mechanism of SiO_2 addition in super-hydrophilic property of TiO_2 films, Surf. Coat. Technol. 173 (2003) 219–223 (See for example).
[5] M. Grätzel, Photoelectrochemical cells, Nature 414 (2001) 338–344.
[6] A. Fujishima, K. Hashimoto, T. Watanabe, TiO_2 Photocatalysis-Fundamentals and Applications, BKC, Tokyo, 1999.
[7] G. Buxbaum, Industrial Inorganic Pigments, Wiley-VCH, Weinheim, 1998.

[8] a R. Garjonyte, A. Malinauskas, L. Gorton, Bioelectrochemistry 61 (2003) 39;
b K.R. Meier, M. Grätzel, Redox targeting of oligonucleotides anchored to nanocrystalline TiO_2 films for DNA detection, ChemPhysChem 3 (2002) 371.
[9] G. Valincius, V. Reipa, M.P. Mayhew, V.L. Vilker, New degenerate metal-oxide electrodes for nearly reversible direct electron transfer to the redox proteins, Electrochem. Commun. 4 (2002) 314–317.
[10] J. Gun, O. Lev O, Sol–gel derived, ferrocenyl-modified silicate-graphite composite electrode: wiring of glucose oxidase, Anal. Chim. Acta 336 (1996) 95–106.
[11] E. Topoglidis, Y. Astuti, F. Duriaux, M. Grätzel, J.R. Durrant, Direct electrochemistry and nitric oxide interaction of heme proteins adsorbed on nanocrystalline tin oxide electrodes, Langmuir 19 (2003) 6894–6900.
[12] E. Topoglidis, C.J. Campbell, A.E.G. Cass, J.R. Durrant, Factors that affect protein adsorption on nanostructured titania films. A novel spectro-electrochemical application to sensing, Langmuir 17 (2001) 7899–7906.
[13] Q.W. Li, G.A. Luo, J. Feng, Direct electron transfer for heme proteins assembled on nanocrystalline TiO_2 film, Electroanalysis 13 (2001) 359–363.
[14] Y. Lvov, B. Munge, O. Giraldo, I. Ichinose, S.L. Suib, J.F. Rusling, Films of manganese oxide nanoparticles with polycations or myoglobin from alternate-layer adsorption, Langmuir 16 (2000) 8850–8857.
[15] M. Collinson, E.F. Bowden, UV–Visible spectroscopy of adsorbed cytochrome-c on tin oxide electrodes, Anal. Chem. 64 (1992) 1470–1476.
[16] X. Chen, S.J. Dong, Sol–gel-derived titanium oxide/ copolymer composite based glucose biosensor, Biosens. Bioelectron. 18 (2003) 999–1004 (See for example).
[17] P.M. Allen, H.A.O. Hill, N.J. Walton, J. Electroanal. Chem. 178 (1984) 69.
[18] R.A. Scott, A.G. Mauk (Eds.), Cytochrome c–a Multidisciplinary Approach, University Science Books, Sausalito, 1996, p 17.
[19] a M. Fedurco, Redox reactions of heme-containing metalloproteins: dynamic effects of self-assembled monolayers on thermodynamics and kinetics of cytochrome *c* electron-transfer reactions, Coord. Chem. Rev. 209 (2000) 263–331;
b M. Kudera, Y. Nakagawa, S. Fletcher, H.A.O. Hill, A voltammetric study of direct electron transfer to cytochrome *c* using a very large assembly of carbon microelectrodes, Lab Chip 1 (2001) 127–131.
[20] K. Miki, T. Ikeda, H. Kinoshita, Electrocatalytic activity of cytochrome *c* for the reduction of nitric oxide, Electroanalysis 6 (1994) 703–705 (See for example).
[21] L. Stryer, Biochemistry, W.H. Freeman and Company, New York, 1995, pp. 541–542. See for example.
[22] K. Niki, W.R. Hardy, M.G. Hill, H. Li, J.R. Sprinkle, E. Margoliash, K. Fujita, R. Tanimura, N. Nakamura, H. Ohno, J.H. Richards, H.B. Gray, Coupling to lysine-13 promotes electron tunneling through carboxylate-terminated alkanethiol self-assembled monolayers to cytochrome *c*, J. Phys. Chem., B 107 (2003) 9947–9949.
[23] X.X. Chen, R. Ferrigno, J. Yang, G.A. Whitesides, Redox properties of cytochrome c adsorbed on self assembled monolayers: a probe for protein conformation and orientation, Langmuir 18 (2002) 7009–7015.
[24] G. Wang, J.J. Xu, H.Y. Chen, Interfacing cytochrome c to electrodes with a DNA carbon nanotube composite film, Electrochem. Commun. 4 (2002) 506–509.
[25] E. Lojou, P. Bianco, Membrane electrodes can modulate the electrochemical response of redox proteins direct electrochemistry of cytochrome *c*, J. Electroanal. Chem. 485 (2000) 71–80.
[26] J.F. Rusling (Ed.), Biomolecular Films, Design, Function, and Applications, Marcel Dekker, New York, 2003, pp. 1–64.
[27] K.J. McKenzie, F. Marken, Accumulation and reactivity of the redox protein cytochrome *c* in mesoporous films of TiO_2 phytate, Langmuir 19 (2003) 4327–4331.
[28] K.J. McKenzie, F. Marken, M. Hyde, R.G. Compton, Nanoporous iron oxide membranes: layer by layer deposition and electrochemical characterisation of processes within nanopores, New J. Chem. 26 (2002) 625–629.
[29] K.J. McKenzie, F. Marken, M. Oyama, C.E. Gardner, J.V. Macpherson, Electrochemistry in the presence of mesoporous TiO_2 phytate nanofilms, Electroanalysis 16 (2004) 89–96.
[30] P.A. Cox, Transition Metal Oxides, Clarendon Press, Oxford, 1995.
[31] G. Garcia-Belmonte, V. Kytin, T. Dittrich, J. Bisquert, Effect of humidity on the ac conductivity of nanoporous TiO_2, J. Appl. Phys. 94 (2003) 5261–5264.
[32] F.L. Qiu, A.C. Fisher, A.B. Walker, L.M. Peter, The distribution of photoinjected electrons a dye sensitized nanocrystalline TiO_2 solar cell modelled by a boundary element method, Electrochem. Commun. 5 (2003) 711–716.
[33] K.J. McKenzie, F. Marken, X. Gao, S.C. Tsang, K.Y. Tam, Quartz crystal microbalance monitoring of density changes in mesoporous TiO_2 phytate films during redox and ion exchange processes, Electrochem. Commun. 5 (2003) 286–291.
[34] F. Scholz, Electroanalytical Methods, Springer, Berlin, 2002, pp. 64–65.
[35] H.A.O. Hill, Y. Nakagawa, F. Marken, R.G. Compton, Voltammetry in the presence of ultrasound: sonovoltammetric detection of cytochrome *c* under very fast mass transport conditions, J. Phys. Chem. 100 (1996) 17395–17399 (See for example).
[36] F. Fabregat Santiago, G. Garcia-Belmonte, J. Bisquert, A. Zaban, P. Salvador, Decoupling of transport, charge storage, and interfacial charge transfer in the nanocrystalline TiO_2/electrolyte system by impedance methods, J. Phys. Chem., B 106 (2002) 334–339 (and reference cited therein).
[37] M.J. Cass, F.L. Qiu, A.B. Walker, A.C. Fisher, L.M. Peter, Influence of grain morphology on electron transport in dye sensitized nanocrystalline solar cells, J. Phys. Chem., B 107 (2003) 113–119.